Performance Analysis of a Two-way Hybrid Photovoltaic/Thermal Solar Collector

H. Mortezapour[1], B. Ghobadian[1*], M. H. Khoshtaghaza[1], and S. Minaei[1]

ABSTRACT

In this paper, the performance evaluation of a two-way hybrid photovoltaic/thermal (PV/T) solar collector was analytically and experimentally carried out. Mathematical expressions for operating parameters in glass to glass and glass to tedlar PV/T solar collectors were developed and experimentally validated by a glass to tedlar PV/T solar collector system. Also the influence of air flow rate on the solar collector performance was investigated. The results showed that the glass to glass PV/T solar collector gave higher outlet air temperature, cell temperature and thermal efficiency than the glass to tedlar PV/T solar collector. However, back surface temperature and electrical efficiency were higher in case of glass to tedlar collector. Increasing the air flow rate led to a lower outlet air temperature and a higher electrical efficiency of the photovoltaic module. Maximum experimental electrical efficiency, thermal efficiency and overall thermal efficiency for the glass to tedlar PV module were found to be 10.35, 57.9 and 84.5%, respectively.

INTRODUCTION

Solar energy is one of the main substitute energy sources for fossil fuels. Photovoltaic cell (PV cell) is the most direct device to convert solar radiation to electricity. More than 80% of solar energy falling on PV cell is absorbed, but it can only convert a maximum of 20% of this energy to electricity (Patel, 2006). The rest of the absorbed energy is converted to heat that increases the cell working temperature and consequently leads to a drop in electrical conversion efficiency. In order to overcome this problem, hybrid photovoltaic/thermal (hybrid PV/T) technology was emerged. In such systems, a fluid (usually air or water) removes the heat from the cell and reduces the cell temperature. After that, the warm outlet fluid is used for other applications such as space or water heating, drying, etc.

Therefore, hybrid PV/T systems simultaneously convert solar radiation to electricity and thermal power. Various researchers have considered the hybrid PV/T system performance and developed electrical and thermal models for PV/T collectors [9, 17, 20, 31]. Chow *et al.* (2006) analyzed energy and exergy of a PV/T collector with and without glass cover. Anderson *et al.* (2009) investigated the performance of a building integrated PV/T solar collector. The effect of fluid flow on energy performance of a hybrid PV/T water heater was investigated by Ji *et al.* (2006). Experimental investigation and modeling of a PV/T solar collector was carried out by Shahsavar and Amiri (2010 who used a thin aluminum sheet suspended at the middle of the solar collector channel to increase the heat exchange surface. Thermal characteristics of a PV module by change of ambient temperature from -25°C to 50°C

[1] Department of Mechanics of Farm Machinery, Faculty of Agriculture, Tarbiat Modares University, Tehran, Islamic Republic of Iran.
[*] Corresponding author; e-mail: ghobadian@modares.ac.ir

were reported by Kim *et al.* (2011) who investigated the effect of using fins attached to the PV module.

Joshi *et al.* (2009) compared thermal performance of two types of PV modules; a glass to glass and a glass to tedlar. In their study, it was reported that the overall thermal efficiency of the glass to glass PV module was 43.4-47.7% more than that of glass to tedlar PV module which was 41.6-45.4%.

Kalogirou (2001) simulated a hybrid PV/T solar system by TRNSYS. An increase in mean annual electrical efficiency of forced mode hybrid PV/T system from 2.8 to 7.7% and a thermal efficiency of 49% was observed. Sarhaddi *et al.* (2010) investigated the thermal and electrical performance of a PV/T solar air collector. A thermal and electrical model was developed and experimentally verified in the above study. The results showed that the thermal, electrical and overall efficiency were 17.18, 10.01 and 45%, respectively. An analytical expression for electrical efficiency of a PV module in various configurations was presented by Dubey *et al.* (2009). The authors reported that the annual average efficiency of glass to glass PV/T collector with and without duct were 10.41 and 9.75%, respectively. Othman *et al.* (2005) analytically performed a double-pass PV/T solar collector with compound parabolic concentrator (CPC) and fins. Their results showed that the electrical efficiency was decreased with increasing temperature of the air flow. Park *et al.* (2010) monitored the performance of a semi-transparent PV module under two various test conditions namely; standard test condition (STC) and outdoor condition. It was observed that the PV module power was decreased about 0.48 and 0.52% per 1°C increase of PV working temperature in STC and outdoor condition, respectively. Tady *et al*. (2008) developed a transient heat model for a building-integrated PV module and verified the model by laboratory tests.

One of the major applications of hybrid PV/T systems in agriculture is agricultural

drying. In these dryers electrical power of PV module usually supplies a DC fan that circulates the air through the collector and drying chamber, and thermal power of the collector is used for heating the flowing air to dry the products [4, 6, 14]. A hybrid PV/T assisted desiccant dryer was designed and evaluated by Punlek *et al.* (2009). Their results showed that drying time and energy consumption in this dryer were reduced compared to hot air drying.

Some of the researchers coupled a heat pump system to a PV/T collector to cool the PV module and consequently achieved a higher electrical efficiency [3, 30]. In such a compound system, a heat pump evaporator was in contact with PV panel which absorbed the heat of panel. The absorbed heat was fed back to the flowing fluid of hybrid PV/T system by a heat pump condenser. Such a system is called "Photovoltaic Solar Assisted Heat Pump PV-SAHP)". Sporn and Ambrose (1995) performed the first experiment on PV-SAHP. Jie *et al.* (2009) evaluated the performance of a PV-SAHP system and presented a mathematical model for energy conversion and experimentally verified the model. Their results indicated that the PV-SAHP system has a coefficient of performance (COP) of 6.5 and electrical efficiency of 13.4%, higher than those of each system individually. Also, Jie *et al.* (2008) developed a distributed dynamic model for a PV-SAHP system. A PV electrical efficiency more than 12% and a thermal efficiency of 50% were observed.

In the literature reviewed so far, one-way or double path PV/T collectors have been considered for investigation. In a one-way collector, the heat carrier fluid was only flowing along one side of the PV module in the collector duct. However, in a double path PV/T collector, the air first flows along one side of the PV panel to the end of the collector, from where the fluid air returns along the other side of PV panel. In this type of collectors, the inlet and outlet ducts are usually positioned on the same side of the collector. In the present investigation, the

performance of a two-way hybrid PV/T solar collector was evaluated. The idea of using this type of collector was developed because in a two-way PV/T solar collector, the air flows along both sides of the PV panel, simultaneously. Therefore, it is expected that the operating parameters of the collector be controlled by adjusting the air flow rate more suitably than both one-way and double path collectors. Performance analysis of a two-way glass to glass and glass to tedlar PV/T solar collector was the main aim of this research. Mathematical expressions were developed to predict the solar cell temperature, back surface temperature, outlet air temperature and electrical and thermal efficiency of both systems. Comparisons of the two models were also performed. Experimental tests were carried out by a two-way hybrid PV/T glass to tedlar under various mass flow rates of flowing air and the experimental measurements were compared with the predicted results.

MATERIALS AND METHODS

Two-way Hybrid PV/T System

Two types of two-way hybrid PV/T systems, glass to glass and glass to tedlar are considered in this study. In a two-way

hybrid PV/T collector, the air flows on both side of the PV module (Figure 1). As it is shown in Figure 1-a, in a two–way hybrid PV/T glass to glass system, solar radiation is absorbed by the solar cell and black surface of bottom insulation partition and heats the solar cell and the insulator. Then thermal convection from both sides of the solar cell and the surface of insulator to the flowing air takes place. In a two-way hybrid PV/T glass to tedlar collector (Figure 1-b) solar radiation is absorbed by the solar cell and tedlar. Then heat is convected from top side of the solar cell and bottom side of tedlar to the flowing air.

In this study, tests were performed in Qaen, a city located in South Khorasan, Iran. The PV solar collector was installed at a tilt angle of 35° equal to the latitude of the city. The solar collector has a wooden duct of dimensions 1.05, 0.805 and 0.1 m that is glazed by a glass layer and the PV module is positioned equidistant from the glazing glass and the bottom insulator of the duct. The bottom insulation consisted of wood and glass wool. A 12V DC fan was used to make the air flow through the duct.

Energy Analysis of PV Solar Collector

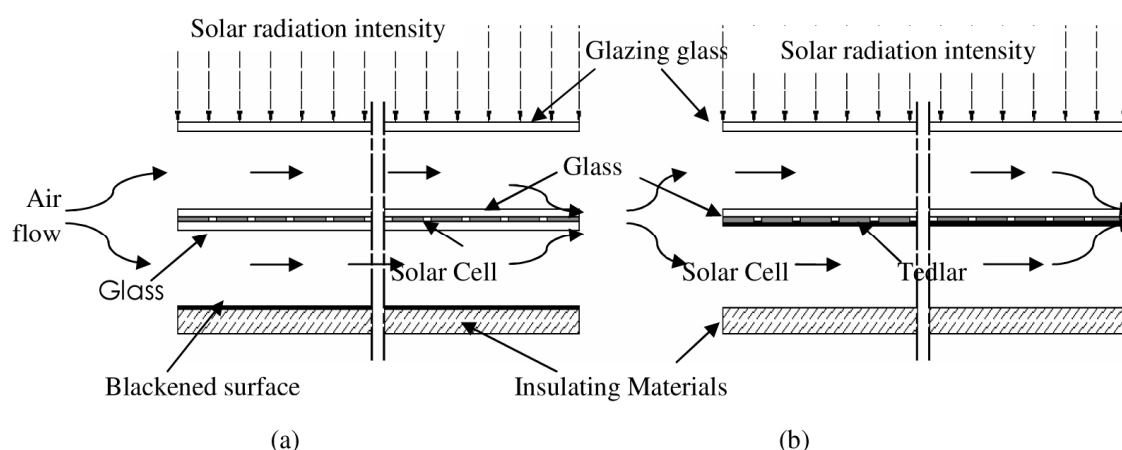The following assumptions were considered to write the energy balance

Figure 1. (a) Schematic view of a two-way glass to glass PV/T collector, (b) Schematic view of a two-way glass to tedlar PV/T collector.

equations of the PV solar collectors:

Thicknesses are very small and temperature variation along the thicknesses is negligible.

The air flow on both sides of PV module is uniform and equal and the air has the same temperature.

The system is in quasi-steady state.

The ohmic losses of the PV module are negligible.

The heat losses from the collector only occur from top and bottom sides.

By considering Dubey *et al.* (2008) and Joshi *et al.* (2009), the following equations for energy balance of each component could be written.

Glass to Tedlar PV Solar Collector

The energy balance equation for the collector is: (equation 1)

By integrating Equation (1) with the initial condition of $T_f = T_{fi}$ at $x = 0$, an equation for flowing air temperature was obtained. (equation 2).

Where

$$(\alpha\tau)_{G-Teff} = \tau_g^2(\alpha_c\beta_c(1-\eta_c) + \alpha_T(1-\beta_c)$$

. If $x = L$ is inserted in Equation (2) the outlet air temperature becomes: (equation 3)

And the average flowing air temperature over the length of PV module is given by: (equation 4)

Thus, the rate of useful thermal energy achieved from PV/T solar collector is:

$$\dot{Q} = \dot{m}_a C_a (T_{fo} - T_{fi}) \qquad (5)$$

After substitution of T_{fo} from Equation (3) in this equation, the rate of useful thermal energy is: (equation 6)

And the thermal efficiency was calculated by the following equation:

$$\eta_{th} = \frac{\dot{Q}}{bLI(t)} \qquad (7)$$

The following energy balance expressions for the solar cell and backside tedlar were written as:

$$(\alpha\tau)_{1,eff} I(t) = h_i(T_c - \bar{T}_f) + U_T(T_c - T_{bs}) \qquad (8)$$

$$[\tau_g^2\alpha_c\beta_c I(t) + \tau_g^2\alpha_T I(t)(1-\beta_c)]bdx = [U_{tf,a}(T_f - T_a) + U_{bf,a}(T_f - T_a) + \tau_g^2\alpha_c\beta_c\eta_c I(t)]bdx + \dot{m}_a C_a \frac{dT_f}{dx}dx \qquad (1)$$

$$T_f = (T_a + \frac{(\alpha\tau)_{G-Teff} I(t)}{U_{tf,a} + U_{bf,a}})(1 - e^{-\frac{(U_{tf,a}+U_{bf,a})x}{\dot{m}_a C_a}}) + T_{fi}e^{-\frac{(U_{tf,a}+U_{bf,a})x}{\dot{m}_a C_a}} \qquad (2)$$

$$T_{fo} = (T_a + \frac{(\alpha\tau)_{G-Teff} I(t)}{U_{tf,a} + U_{bf,a}})(1 - e^{-\frac{(U_{tf,a}+U_{bf,a})L}{\dot{m}_a C_a}}) + T_{fi}e^{-\frac{(U_{tf,a}+U_{bf,a})L}{\dot{m}_a C_a}} \qquad (3)$$

$$\bar{T}_f = \frac{1}{L}\int_0^L T_f dx = (T_a + \frac{(\alpha\tau)_{G-Teff} I(t)}{U_{tf,a} + U_{bf,a}})(1 - \frac{1 - e^{-\frac{(U_{tf,a}+U_{bf,a})L}{\dot{m}_a C_a}}}{L}) + (T_{fi}\frac{1 - e^{-\frac{(U_{tf,a}+U_{bf,a})L}{\dot{m}_a C_a}}}{\frac{U_{tf,a} + U_{bf,a}}{\dot{m}_a C_a}}) \qquad (4)$$

$$\dot{Q} = \dot{m}_a C_a((T_a + \frac{(\alpha\tau)_{G-Teff} I(t)}{U_{tf,a} + U_{bf,a}})(1 - \frac{1 - e^{-\frac{(U_{tf,a}+U_{bf,a})L}{\dot{m}_a C_a}}}{L}) + T_{fi}(\frac{1 - e^{-\frac{(U_{tf,a}+U_{bf,a})L}{\dot{m}_a C_a}}}{-\frac{(U_{tf,a}+U_{bf,a})}{\dot{m}_a C_a}} - 1)) \qquad (6)$$

$$(\alpha\tau)_{2,eff} I(t) + U_T(T_c - T_{bs}) = h_i(T_c - \bar{T}_f) \tag{9}$$

Where $(\alpha\tau)_{1,eff} = \tau_g^2 \alpha_c \beta_c (1 - \eta_c)$

and $(\alpha\tau)_{2,eff} = \tau_g^2 \alpha_T (1 - \beta_c)$.

The solution for these two equations with substituting T_f gives the solar cell temperature (T_c) and backside temperature (T_{bs}): (equations 10 and 11)

The following expression for the electrical efficiency was used [12, 13, 26]

$$\eta_{el} = \eta_0[1 - 0.0045(T_c - 25)] \tag{12}$$

By substituting T_c from Equation (10), in Equation (12), the electrical efficiency of PV module was calculated. Electrical efficiency was converted to thermal efficiency equivalent by using the following equation:

$$\eta_{el,th} = \frac{\eta_{el}}{C_f} \tag{13}$$

Finally, overall thermal efficiency was obtained by adding the thermal efficiency from Equation (6) and thermal efficiency equivalent from Equation (13):

$$\eta_{overall} = \eta_{th} + \eta_{el,th} \tag{14}$$

Glass to glass PV Solar Collector

By modifying Joshi *et al.* (2009) equations, the following general energy balance equation was written for the glass to glass PV/T solar collector. (equation 15)

Where $(\alpha\tau)_{3,eff} = \alpha_p (1 - \beta_c)\tau_g^3$. The energy balance equation for back surface is: (equation 16)

Back surface temperature was calculated from Equation (16):

$$T_{bs} = \frac{(\alpha\tau)_{3,eff} I(t) + h_i T_f + U_{bs,a} T_a}{U_{bs,a} + h_i} \tag{17}$$

By the substitution of T_{bs} from Equation (17), in Equation (15) and integrating this equation with the boundary condition, $T_f = T_{fi}$ at $x = 0$, the flowing air temperature was obtained by: (equation 18)

where $HP_1 = \frac{U_{bs,a}}{U_{bs,a} + h_i}$. By substituting $x = L$ in Equation (18), the outlet air temperature was calculated. The average air temperature over the length of PV module was used by the following equation 19:

$$T_c = \frac{(\alpha\tau)_{1,eff} I(t) - (\alpha\tau)_{2,eff} I(t)}{h_i + 2U_T}(\frac{U_T}{h_i} + 1) + \frac{(\alpha\tau)_{2,eff} I(t)}{h_i} \tag{10}$$

$$T_{bs} = \frac{(\alpha\tau)_{2,eff} I(t)}{h_i} + \frac{U_T}{h_i}(\frac{(\alpha\tau)_{1,eff} I(t) - (\alpha\tau)_{2,eff} I(t)}{h_i + 2U_T}) + \bar{T}_f \tag{11}$$

$$[(\alpha\tau)_{1,eff} I(t) + (\alpha\tau)_{3,eff} I(t)]bdx = \dot{m}_a C_a \frac{dT_f}{dx} dx + [U_{tf,a}(T_f - T_a) + U_{bs,a}(T_{bs} - T_a)]bdx \tag{15}$$

$$(\alpha\tau)_{3,eff} I(t)bdx = [h_i(T_{bs} - T_f) + U_{bs,a}(T_{bs} - T_a)] \tag{16}$$

$$T_f = \frac{[((\alpha\tau)_{1,eff} + (\alpha\tau)_{3,eff} - HP_1(\alpha\tau)_{3,eff})I(t) + T_a(U_{tf,a} + U_{bs,a} - HP_1 U_{bs,a})]}{(HP_1 h_i + U_{fa})}) +$$

$$(T_{fi} - \frac{[((\alpha\tau)_{1,eff} + (\alpha\tau)_{3,eff} - HP_1(\alpha\tau)_{3,eff})I(t) + T_a(U_{tf,a} + U_{bs,a} - HP_1 U_{bs,a})]}{(HP_1 h_i + U_{fa})}).e^{-\frac{(HP_1 h_i + U_{tf,a}).b}{\dot{m}_a C_a}x}$$

$$\tag{18}$$

$$\bar{T}_f = \frac{1}{L}\int_0^L T_f dx = \frac{[((\alpha\tau)_{1,eff} + (\alpha\tau)_{3,eff} - HP_1(\alpha\tau)_{3,eff})I(t) + T_a(U_{tf,a} + U_{bs,a} - HP_1 U_{bs,a})]}{(HP_1 h_i + U_{tf,a})}$$

$$+ \frac{1}{\frac{(HP_1 h_i + U_{tf,a}).b}{\dot{m}_a C_a}L}(T_{fi} - \frac{[((\alpha\tau)_{1,eff} + (\alpha\tau)_{3,eff} - HP_1(\alpha\tau)_{3,eff})I(t) + T_a(U_{tf,a} + U_{bs,a} - HP_1 U_{bs,a})]}{(HP_1 h_i + U_{tf,a})})$$

$$(1 - e^{\frac{(HP_1 h_i + U_{tf,a}).b}{\dot{m}_a C_a}L})$$

$$\tag{19}$$

$$[\alpha_c \tau_g^2 \beta_c I(t)]b.dx = [2U_{cf}(T_c - \bar{T}_f) + \tau_g^2 \eta \alpha_c \beta_c I(t)]b.dx \tag{20}$$

The following energy balance expression for solar cell was written as: (equation 20)

Simplifying Eq. (20) for T_c, gives the next equation for solar cell temperature.

$$T_c = \bar{T}_f + \frac{(\alpha\tau)_{1,eff} I(t)}{2U_{cf}} \tag{21}$$

By substituting $\bar{T}_f$ from Equation (19) in Equation (21), the solar cell temperature was obtained.

Finally, by the substitution of T_{fo} and T_c in Equations (5) and (12), respectively and by using Equations (13) and (14) the useful thermal energy, thermal efficiency, thermal efficiency equivalent and overall thermal efficiency were calculated.

Experimentation and Measurement

The tests were carried out in the month of August from 9 am to 15 pm. The PV module was a single-crystalline silicone (AS 120) and its characteristics at standard testing condition were: open circuit voltage V_{oc}= 30V, short-circuit current I_{sc}= 4A, electrical efficiency η_o =12%. Two temperature sensors were positioned in front and on the back surface of the PV module to measure cell and back surface temperature. In order to measure the temperature of inlet and outlet flowing, two temperature sensors (SMT 160) were installed before and after the collector duct. Simultaneously, a solar power meter (TES 1333R) measured the solar radiation intensity on the collector surface, during the test. A multimeter (DEC 330FC) was used to measure the open circuit voltage (V_{oc}) and short circuit current (Isc). Experimental efficiency of the PV module was calculated (Geotzberger and Hoffmann, 2005):

$$\eta_{exp} = \frac{FF \times V_{oc} \times I_{sc}}{A \times I_{(t)}} \tag{22}$$

The design parameters of the PV/T solar collector used in this study are listed in Table 1. The values of $K_g, \tau_g, \alpha_c, K_T, \alpha_p$ and C_f in this table are taken from [1, 8, 11, 23]. Meanwhile, the following relations were used to define the heat transfer coefficients in the study:

$$h_i = 2.8 + 3v_i \tag{23}$$

$$h_o = 5.7 + 3.8v_i \tag{24}$$

$$U_{bf,a} = [\frac{1}{h_i} + \frac{l_w}{K_w} + \frac{l_{gw}}{K_{gw}} + \frac{1}{h_o}]^{-1} \tag{25}$$

$$U_{tf,a} = [\frac{1}{h_i} + \frac{l_{gg}}{K_g} + \frac{1}{h_o}]^{-1} \tag{26}$$

$$U_T = [\frac{l_T}{K_T}]^{-1} \tag{27}$$

$$U_{bs,a} = [\frac{l_w}{K_w} + \frac{l_{gw}}{K_{gw}} + \frac{1}{h_o}]^{-1} \tag{28}$$

$$U_{cf} = [\frac{l_g}{K_g} + \frac{1}{h_i}]^{-1} \tag{29}$$

(r)

Table 1. Design parameters of PV/T solar collector.

Parameters	Values
Length of PV module (L)	1.05 m
Width of PV module (b)	0.805 m
Duct depth (d)	0.9 m
Packing factor of solar cell $(\beta_c)^a$	0.83
Thickness of glass cover (l_g)	0.003 m
Conductivity of glass cover (K_g)	1 W mK^{-1}
Transmissivity of glass cover (τ_g)	0.95
Thickness of glazing glass ($l_{g.g}$)	0.005 m
Absorptivity of solar cell (α_c)	0.83
Fill factor (ff)**	0.8
Absorptivity of blackened surface (α_p)	0.8
Absorptivity of tedlar (α_T)	0.5
Thickness of tedlar (l_T)	0.0005 m
Conductivity of tedlar (K_T)	0.033 W mK^{-1}
Thickness of back wooden insulation (l_w)	0.02 m
Conductivity of back wooden insulation (K_w)	0.13 W mK^{-1}
Thickness of back glass wool insulation ($l_{g.w}$)	0.025 m
Conductivity of back glass wool insulation($K_{g.w}$)	0.004 W mK^{-1}
Conversion factor of the thermal power plant (C_f)	0.36
Wind speed (v_w)	0.5 m/s

** The fill factor is reasonably constant for a wide range of values of the irradiance and close to 0.8, [5].
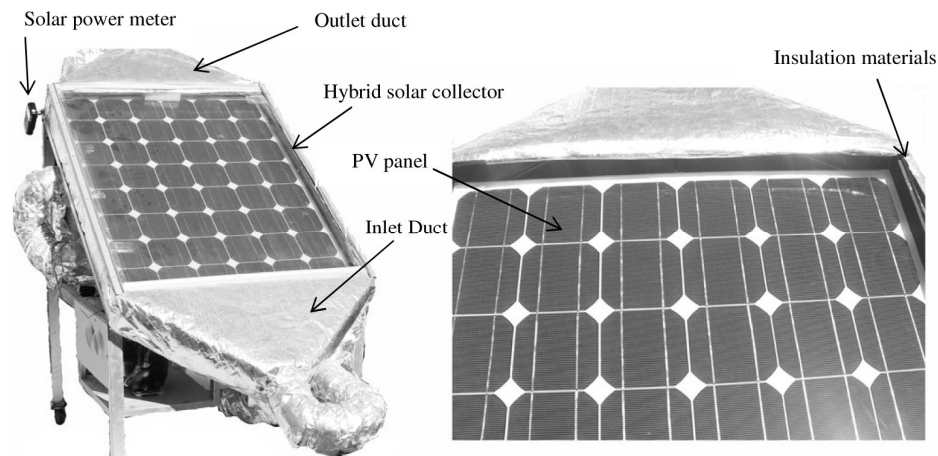

Figure 2. (a) Photograph of the experimental setup of hybrid PV/T solar collector and (b) Close view to the two-way PV/T solar collector structure.

A photograph of the experimental setup of two-way PV/T collector of the present study is shown in Figure 2.

Experimental Validation

To compare the theoretical and experimental results and also to validate the derived equations, the correlation coefficient and the root mean square percent deviation (e) were evaluated using the following equations:

$$r = \frac{N\sum X_i Y_i - (\sum X_i)(\sum Y_i)}{\sqrt{N\sum X_i^2 - (\sum X_i)^2}\sqrt{N\sum Y_i^2 - (\sum Y_i)^2}}$$

(30)

and

$$e = \sqrt{\frac{\sum (e_i)^2}{N}}$$

(31)

773

where $e_i = [\dfrac{X_i - Y_i}{X_i}]$.

Also, the means of theoretical and experimental data are compared by *t*-Test method. This comparison was carried out by SPSS software.

RESULTS AND DISCUSSION

The hourly variation of solar radiation intensity and ambient air temperature for a typical day of August 2010 under the conditions of Qaen, from 9 am to 3 pm are shown in Figure 3 The solar radiation intensity varies from 712 W m^{-2} at 9 am to 1050 W m^{-2} at 12 Noon and the ambient air temperature is in the range of 27.3°C at 9 am to 33.4°C at 1pm.

In order to validate the theoretical calculations experimentally, experimental and theoretical outlet air temperature, back surface temperature, cell temperature and electrical

efficiency under typical solar intensity, ambient air temperature, inlet air temperature and air mass flow rate of 0.05 kg/s, are shown in Figure 4.

As it is indicated, the mean square deviation is between 2.83 and 5.35% and the value of linear correlation coefficient is between 0.8080 and 0.9969. Therefore, it can be said that there is a fair agreement between experimental and theoretical results. Although, it is clear that experimental and theoretical results for outlet air temperature is closer than three other parameters. It is found that as the cell temperature increases, the electrical efficiency of PV module decreases. Experimental results also indicated that electrical efficiency of glass to tedlar PV/T solar collector varies from 9.46% to 10.35%.

The results of means comparison by *t*-Test method for the theoretical and experimental outlet air temperature, back surface temperature, cell temperature and electrical efficiency are presented in Table 2. It was observed that there was no significant
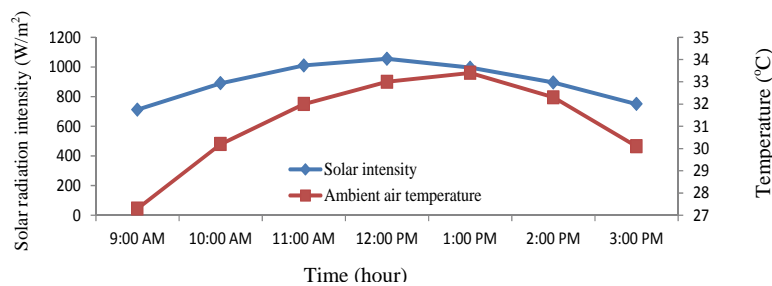

Figure 3. Hourly variation of solar radiation intensity and ambient air temperature for a typical day of August 2010 under the conditions of Qaen.

Table 2. Comparison of the means of theoretical and experimental data by *t*-Test method.

Parameter	Data type	Mean	Std. deviation	Mean difference	Std. error difference	df	*t* value
Outlet air temperature	Theoretical	48.7	6.55	1.2875	2.80954	21.813	0.458 [ns]
	Experimental	47.4	7.19				
Cell temperature	Theoretical	70.5	7.92	-04250	3.65281	21.027	-0.116 [ns]
	Experimental	71	9.86				
Back surface temperature	Theoretical	67.4	7.51	-1.0483	3.61929	20.394	-0.290 [ns]
	Experimental	68.5	10.03				
Electrical efficiency	Theoretical	9.69	0.43	-0.104	0.148	18.651	-0.699 [ns]
	Experimental	9.8	0.27				

[ns]: Indicates no significant difference between the means of the two groups.

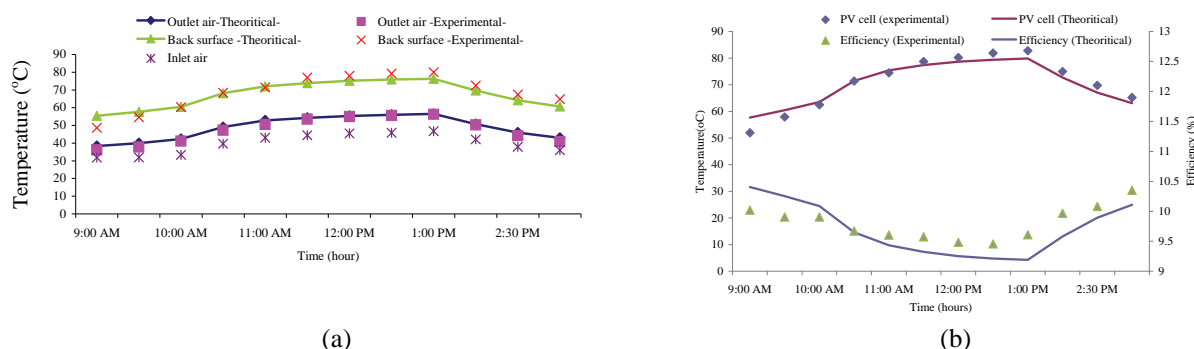(a)   (b)

Figure 4. (a) Hourly variation of inlet air temperature and experimental validation of outlet air temperature back surface temperature for the glass to tedlar PV/T solar collector, (b) Experimental validation of the solar cell temperature and electrical efficiency for the glass to tedlar PV/T solar collector.
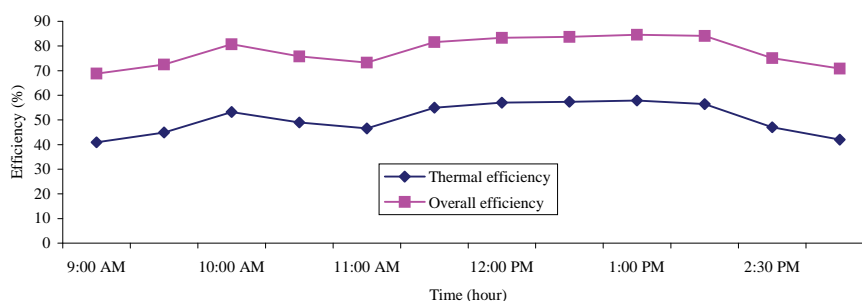

Figure 5. Experimental hourly variation of thermal and overall thermal efficiency of the glass to tedlar PV/T solar collector.

difference between the means of theoretical and experimental data for any of the parameters.

Thermal and overall thermal efficiency ware calculated by using Equations (7) and (14) and with the above experimental data of glass to tedlar PV/T module and the results are shown in Figure 5. Thermal efficiency ranged between 40.9 and 57.9% whereas overall thermal efficiency ranged between 68.7 and 84.5%.

Figure 6 shows outlet air temperature, back surface temperature, cell temperature and electrical efficiency of glass to tedlar PV/T solar collector under three air mass flow rates of 0.02, 0.035 and 0.05 kg s^{-1}. It is clear that when the air flow rate increases, the outlet air temperature, back surface temperature and cell temperature decrease while the electrical efficiency increases. That is because, by increasing the air flow rate, the velocity of air in the solar collector

increases and consequently the time during which air flows through the collector decreases and therefore, the air leaves the duct at a lower temperature. As a result, it can be concluded that when air flow rate increases the outlet air temperature and therefore the average air temperature over the length of the collector decreases. This is in agreement with the results obtained by Dubey *et al.* (2009). The cooler air temperature in the collector causes a lower temperature of back surface and cell and consequently a higher electrical efficiency of the PV module. Equations (15) to (21) were used for the glass to glass PV/T solar collector calculations. Figure 7 shows variation of the collector parameters for both glass to tedlar and glass to glass PV/T solar collectors. Outlet air temperature of glass to glass PV/T collector is slightly higher than that of glass to tedlar one. This is because the black surface of the glass to glass PV/T
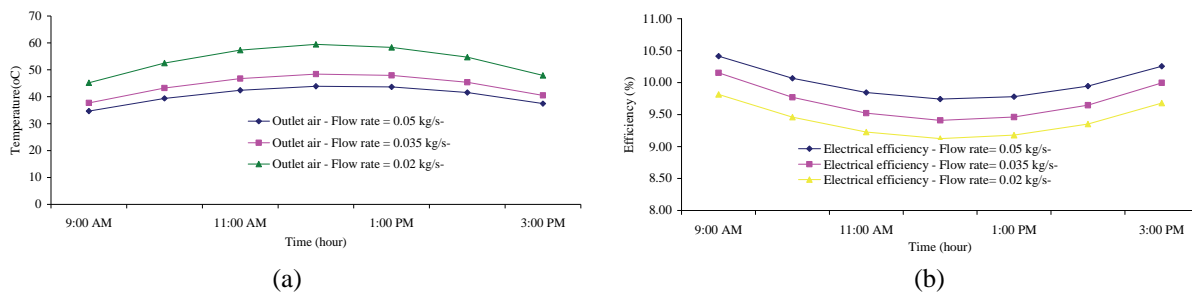
775

(a)

(b)

Figure 6. Comparison of the influence of the various air flow rates on parameters: (a) outlet air temperature and (b) electrical efficiency.
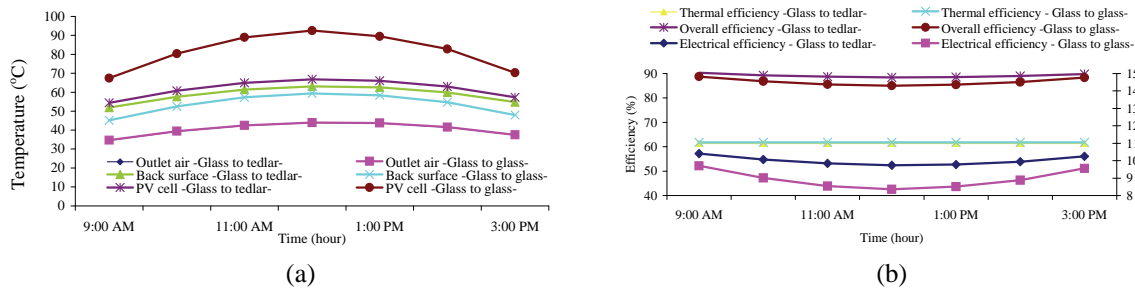

(a)

(b)

Figure 7. (a) Hourly variations of outlet air temperature, back surface temperature and solar cell temperature for both glass to glass and glass to tedlar PV/T solar collector. (b) Hourly variations of electrical, thermal and overall thermal efficiency for both glass to glass and glass to tedlar PV/T solar collector.

collector absorbs more solar energy than tedlar surface of the glass to tedlar PV/T collector. Therefore, total available thermal energy is higher in glass to glass than glass to tedlar PV/T collector. This finding is in accordance with the results of Joshi *et al.* (2009). Similarly from Figure 7 it is clear that the cell temperature is higher in case of glass to glass collector.

On the contrary, the back surface temperature is lower in case of glass to glass collector. This finding contradics the results of Joshi *et al.* (2009). This maybe because the available thermal energy on PV cell is conducted from back side to tedlar in both one-way and two-way glass to tedlar PV/T solar collectors whereas in the case of one-way collector, heat is convected from top surface to ambient air. In a two-way collector, heat is convected from top side to inside flowing air. However, because the convection coefficient of the flowing air in this study is lower than ambient convection coefficient, heat transfer from cell to tedlar

is more than that from cell to flowing air. It is clear that if the air velocity inside the solar collector increases adequately as its convection coefficient becomes more than the convection coefficient of the ambient air, then the back surface temperature will be higher in glass to glass than glass to tedlar PV/T collector.

The variations of thermal, overall and electrical efficiency for both glass to tedlar and glass to glass PV/T collectors are shown in Figure 7-b.

Because of the higher outlet air temperature and cell temperature of the glass to glass PV/T collector, it has a higher thermal efficiency and a lower electrical efficiency than the glass to tedlar PV/T collector. It is found that the overall thermal efficiency is higher in case of glass to tedlar collector. That is because of higher electrical efficiency of glass to tedlar PV/T collector that lest to a thermal efficiency equivalent more than the glass to glass PV/T collector.

CONCLUSIONS

In this study, electrical and thermal analysis of a two-way hybrid photovoltaic/thermal solar collector was performed and mathematical models were developed for glass to tedlar and glass to glass PV/T solar collectors. Briefly, the following conclusions were derived:

Experimental validation for glass to tedlar PV/T solar collector was performed and it was found that there was a good agreement between theoretical and experimental results.

Maximum experimental electrical, thermal and overall thermal efficiencies for glass to tedlar PV module were found to be 10.35, 57.9 and 84.5%, respectively.

Outlet air temperature, back surface temperature and cell temperature while decreased and electrical efficiency increased when the air mass flow rate increased.

Glass to glass PV/T solar collector experienced higher outlet air temperature, cell temperature and thermal efficiency than glass to tedlar PV/T solar collector whereas back surface temperature and electrical efficiency were higher in case of glass to tedlar collector.

Finally, the overall thermal efficiency of glass to tedlar PV module was more than overall efficiency of glass to glass PV module.

Nomenclature

A	Area	m^2
B	Width of collector	m
C_a	Specific heat of air	J/kg K
C_f	The conversion factor of thermal power plant	
D	Depth of collector duct	m
dx	Elemental length	m
e	Root mean square percentage deviation	%
FF	Fill factor	
h_i	Heat convective coefficient of inside air	W/m^2 K
h_o	Heat convective coefficient of ambient air	W/m^2 K
I_{sc}	Short-circuit current	A
$I(t)$	Solar radiation intensity	W/m^2
L	Length of collector	m
$\dot{m}_a$	Mass flow rate of air	kg/s
N	Number of experimental/predicted data	
$\dot{Q}$	Rate of useful energy	W
r	Linear coefficient of correlation	
T_a	Ambient air temperature	^{o}C
T_{bs}	Back surface temperature	^{o}C
T_c	Solar cell temperature	^{o}C
T_f	Flowing air temperature	^{o}C
$\overline{T}_f$	Average air temperature over the length of PV module	^{o}C
T_{fi}	Inlet air temperature	^{o}C
T_{fo}	Outlet air temperature	^{o}C
$U_{bf,a}$	An overall back loss coefficient from back way flowing air to ambient	W/m^2 K
$U_{bs,a}$	An overall heat loss coefficient from the back surface to air collector to the environment	W/m^2 K
U_{cf}	An overall heat loss coefficient from the PV/T air collector to the environment	W/m^2 K
$U_{tf,a}$	An overall heat loss coefficient from top way flowing air to ambient	W/m^2 K
U_T	An overall heat loss coefficient from the solar cell to tedlar	W/m^2 K
V_{oc}	Open-circuit voltage	V
X_i	theoretical data	
Y_i	Experimental data	
α_c	Absorptivity of solar cell	
α_p	Absorptivity of black surface	
$(\alpha\tau)_{G-Teff}$	Product of effective absorptivity and transmissivity on cell and tedlar	
$(\alpha\tau)_{1.eff}$	Product of effective absorptivity and transmittivity on cell	
$(\alpha\tau)_{2.eff}$	Product of effective absorptivity and transmittivity on tedlar	
$(\alpha\tau)_{3.eff}$	Product of effective absorptivity and	

β_c	transmittivity on back plate Packing factor of solar cell	
η_0	Solar cell efficiency at standard testing condition (STC)	%
η_c	Solar cell efficiency	%
$\eta_{el,th}$	Thermal efficiency equivalent of electrical efficiency	%
η_{el}	Electrical efficiency	%
η_{exp}	Experimental electrical efficiency	%
η_{overal}	Overall thermal efficiency	%
η_{th}	Thermal efficiency	%
τ_g	Transitivity of glass	

REFERENCES

1. Anderson, T. N., Duke, M, Morrison G. L. and Carson, J. K. 2009. Performance of a Building Integrated Photovoltaic/Thermal (BIPVT) Solar Collector. *Sol. Energy*, **84:** 445-455.

2. Anonymous 2004. A Strategy for Growth of Electrical Energy in India: Document 10. Department of Atomic Energy, Government of India, http://www.dae.gov.in/publ/doc10/index.htm.

3. Badescu, V. 2003. Model of a Thermal Energy Storage Device Integrated into a Solar Assisted Heat Pump System for Space Heating, *Energy Convers. Manage.,* **44:** 1589–1604.

4. Barnwal, P. and Tiwari, G. N. 2008. Grape Drying By Using Hybrid Photovoltaic-Thermal (PV/T) Greenhouse Dryer: An Experimental Study. *Sol. Energy*, **82:** 1131-1144.

5. Castaner, L. and Silvester, S. 2002. *Modeling photovoltaic Systems Using PSpice*. John Willy and Sons Ltd., South Gate, Chichester, England. 358 P.

6. Chen, H. H., Hernandez, C. E. and Huang, T. C. 2005. A Study of The Drying Effect on Lemon Slices Using a Closed-Type Solar Dryer. *Sol. Energy*, **78:** 97–103.

7. Chow, T. T., He, W. and Ji, J. 2006. Hybrid Photovoltaic-Thermosyphon Water Heating System for Residential Application. *Sol. Energy*, **80:** 298–306.

8. Dubey, S., Sandhu, G. S. and Tiwari, G. N. 2009. Analytical Expression for Electrical Efficiency of PV/T Hybrid Air Collector. *App. Energy*, **86:** 697-705.

9. Dubey, S., Solanki, S. C. and Tiwari, A. 2009. Energy and Exergy Analysis of PV/T Air Collectors Connected in Series, *Energ. Buildings*, **41:** 863-870.

10. Dubey, S. and Tiwari, G. N. 2008. Thermal modeling of a Combined System of Photovoltaic Thermal (PV/T) Solar Water Heater. *Sol. Energy* **82:** 602–612.

11. Duffie, J. A. and Beckman, W. A. 2006. *Solar Engineering of Thermal Processes.* Wiley, New York. 908P.

12. Evans, L. 1981. Simplified Method for Predicting PV Array Output. *Sol. Energy*, **27:** 555–560.

13. Geotzberger, A. and Hoffmann, V. U. 2005. *Photovoltaic Solar Energy Generation.* Springer Berlin Heidelberg New York. 235P.

14. Hossain, M. A. and Bala, B. K. 2007. Drying of Hot Chilli Using Solar Tunnel Dryer. *Sol. Energy*, **81:** 85–92.

15. Ji, J., Han, J., Chow T. T., Yi, H., Lu, J., He, W. and Sun, W. 2006. Effect of Fluid Flow and Packing Factor on Energy Performance of Wall-Mounted Hybrid Photovoltaic/Water-Heating Collector System, *Energ. Building*, **83:** 1380-1387.

16. Ji, J., He, H., Chow, T., Pei, G., He, W. and Liu, K. 2009. Distributed Dynamic Modeling and Experimental Study of PV Evaporator in a PV/T Solar-assisted Heat Pump, *Int. J. Heat Mass Tran.* **52:** 1365-1373.

17. Ji, J., Pei, G., Chow, T. T., Liu, K., He, H., Lu, J. and Han, C. 2008. Experimental Study of Photovoltaic Solar Assisted Heat Pump System. *Sol. Energy*, **82:** 43-52.

18. Joshi, A. S., Tiwari, A., Tiwari, G. N., Dincer, I. and Reddy, B. V. 2009. Performance Evaluation of a Hybrid Photovoltaic Thermal (PV/T) (Glass-to-Glass) System. *Int. J. Therm. Sci.*, **48:** 154-164.

19. Kalogirou, S. A. 2001. Use of TRYNSYS for Modeling and Simulation of a Hybrid PV-thermal Solar System for Cyprus. *Renew. Energy*, **23:** 247–260.

20. Kim, J. P., Lim, H., Hun Song, J. H., Chang, Y. J. and Jeon, C. H. 2011. Numerical Analysis on the Thermal Characteristics of Photovoltaic Module with Ambient

Temperature Variation. Sol. _Energy Mat. Sol. C._,**95**: 404-407.

21. Othman, M. Y. H., Yatim, B., Sopian, K. and Nazari Abu Bakar, M. 2005. Performance Analysis of a Double-Pass Photovoltaic/Thermal (PV/T) Solar Collector with CPC and Fins. _Renew. Energy_ **30**: 2005-2017.

22. Park, K. E., Kang, G. H., Kim, H. I., Yu, G. J. and Kim, J. T. 2010. Analysis of Thermal and Electrical Performance of Semi-transparent Photovoltaic (PV) Module. _Energy_, **35**: 2681-2687.

23. Patel, M. R. 2006. _Wind and Solar Power Systems._ Taylor and Francis group, 447P.

24. Punlek, C., Pairintra, R., Chindaraksa, S. and Maneewan, S. 2009. Simulation Design and Evaluation of Hybrid PV/T Assisted Desiccant Integrated HA-IR Drying System (HPIRD). _Food Bioprod. Process._, **87**: 77-86.

25. Sarhaddi, F., Farahat, S., Ajam, H., Behzadmehr, A. and MahdaviAdeli, M. 2010. An Improved Thermal and Electrical Model for a Solar Photovoltaic Thermal (PV/T) Air Collector. _Appl. Energy_, **87**: 2328-2339.

26. Schott, T. 1985. Operational Temperatures of PV Modules. In: _Proceedings of 6th PV Solar Energy Conference,_ April 15-19, 1985, London, PP. 392–396.

27. Shahsavar, A. and Amiri, M. 2010. Experimental Investigation and Modeling of a Direct-coupled PV/T Air Collector. _Sol. Energy_ **84**: 1938-1958.

28. Sporn, P. and Ambrose, E. R. 1995. The Heat Pump and Solar Energy. _Proceedings of the World Symposium on Applied Solar Energy_, November 1-5, 1995, Phoenix, Arizona, 159-170.

29. Tady, Y., Fung, Y. and Yang, H. 2008. Study on Thermal Performance of Semi-transparent Building-integrated Photovoltaic Glazings. _Energ. Buildings_, **40**: 341-350.

30. Xu, G., Deng, S., Zhang, X., Yang, L. and Zhang, Y. 2009. Simulation of a Photovoltaic/Thermal Heat Pump System Having a Modified Collector/Evaporator. _Sol. Energy_, **83**: 1967-1976.

31. Zogou, O. and Stapountzis, H. 2011. Energy Analysis of an Improved Concept of Integrated PV Panels in an Office Building in Central Greece. _Appl. Energy_, **88**: 853-866.

بررسی عملکرد جمع‌کننده خورشیدی ترکیبی فتوولتائیک-گرمایی دوراهه

ح. مرتضی پور، ب. قبادیان، م. ه. خوش تقاضا و س. مینائی

چکیده

در تحقیق حاضر، عملکرد یک جمع‌کننده خورشیدی ترکیبی فتوولتائیک-گرمایی به به صورت تئوری و تجربی بررسی گردید. معادلات ریاضی برای دو نوع جمع‌کننده ترکیبی فتوولتائیک-گرمایی شیشه به شیشه و شیشه به تدلار ارائه شد و درستی معادلات ریاضی، برای نوع شیشه به تدلار توسط آزمایش‌های تجربی بررسی گردید. همچنین، تاثیر تغییر دبی هوای عبوری بر عملکرد جمع‌کننده خورشیدی ترکیبی مطالعه شد. نتایج نشان دادند که در جمع‌کننده نوع شیشه به شیشه، دمای هوای خروجی، دمای سلول و بازده حرارتی نسبت به نوع شیشه به تدلار بیشتر است. اما، دمای سطح پشتی و بازده الکتریکی در جمع‌کننده ترکیبی شیشه به تدلار بشتر از نوع شیشه به شیشه بود. افزایش دبی هوای عبوری باعث افزایش بازده الکتریکی گردید. در نهایت، بیشترین بازده الکتریکی، حرارتی و کلی در

779

جمع‌کننده خورشیدی ترکیبی فتوولتائیک-گرمایی نوع شیشه به تدلار به صورت تجربی، به ترتیب ۱۰/۳۵، ۵۷/۹ و ۸۴/۵ درصد به‌دست آمد.